Food Biophysics (2010) 5:218–226
DOI 10.1007/s11483-010-9163-2

ORIGINAL ARTICLE

Pre-nucleation Structuring of Triacylglycerols and Its Effect on the Activation Energy of Nucleation

Elena Dibildox-Alvarado · Alejandro G. Marangoni · Jorge F. Toro-Vazquez

Published online: 28 May 2010

Abstract Based in a previous study involving anisotropy measurements (r_s) and molecular mechanics simulations, we investigated the molecular interaction occurring among triacylglycerols (TAGS) before their nucleation, and its possible involvement in determining the activation free energy to develop a stable nucleus (ΔG_c). The Fisher-Turnbull equation was used to calculate the ΔG_c involved in the nucleation of tripalmitin (TP) or tristearin (TS) blended in a 25:75 ratio with triolein (TO), high oleic safflower oil (HOSfO), and soybean oil (SBO). The crystallization temperatures used were selected to obtain similar supercooling conditions in all blends investigated. As our previous study showed, the anisotropy measurements (r_s) showed that TAGS with at least one chain of palmitic acid (i.e., POO, LLP, PLO) induce TAGS' pre-nucleation structuring in both the TP and TS blends. However, for TS blends, the molecular interaction occurred well before attaining supercooling conditions required for crystallization (i.e., during the cooling stage). Once these supercooling conditions were achieved, TAGS with palmitic acid acted as template for TS crystallization. As a result, ΔG_c in TS/HOSfO and TS/SBO blends were lower than the ΔG_c in the TS/TO blend. In contrast, in the TP blends TAGS structuring (i.e., an increase in r_s) occurred as a function of time under isothermal conditions as a direct function of the concentration of TAGS containing at least one chain of palmitic acid. We postulate that the molecular interactions occurring in the liquid phase between TP and TAGS with palmitic acid, resulted in the development of a mixed TAGS lamellar liquid structure. This delayed TP nucleation until segregation of TP from the mixed TAGS lamellar liquid structure occurred. This resulted in a higher ΔG_c for TP nucleation as the concentration of LLP, POO, PLO, and PLO increased in the blends. The molecular interactions occurring among TAGS in the liquid phase under supercooling conditions must be understood, since they directly relate to the TAGS crystallization process that in turns determines the macroscopic properties evaluated by consumer in lipid-based products. The results presented in this manuscript are in this line of investigation.

Keywords Pre-nucleation structuring · Triacylglycerols structuring · Fisher-Turnbull · Anisotropy · Triacylglycerols nucleation

E. Dibildox-Alvarado · J. F. Toro-Vazquez
Universidad Autonoma de San Luis Potosi,
Facultad de Ciencias Quimicas,
San Luis Potosi, Mexico

E. Dibildox-Alvarado
Universidad Autonoma de Queretaro, DIPA-PROPAC,
Santiago de Querétaro, Mexico

A. G. Marangoni
University of Guelph, Department of Food Science,
Guelph, Canada

J. F. Toro-Vazquez (✉)
Facultad de Ciencias Químicas-CIEP,
Av. Dr. Manuel Nava 6, Zona Universitaria,
San Luis Potosí, SLP 78210, Mexico
e-mail: toro@uaslp.mx

Introduction

Vegetable oils and fats are multicomponent systems containing different families of triacylglycerols (TAGS). In these systems, the molecular relationships occurring among TAGS families determine the thermodynamic conditions (i.e., supercooling and supersaturation) that drive the formation of a solid from the liquid phase, the organization

of the solid phase, and its phase behavior. The resulting three-dimensional TAGS crystal network and the phase behavior of TAGS are major factors determining the physical and functional properties (i.e., rheology, liquid phase entrapment, mouthfeel, appearance, and spreadability) in products such as margarine, butter, confectionary coatings, and fillings[1]. Thus, the complex molecular interactions occurring among TAGS in the liquid phase under supercooling conditions must be first understood, since they directly relate to the TAGS crystallization process that in turns determines the macroscopic properties evaluated by consumer in vegetable oil and fat-based products.

Nematic[2], smectic[3], and discotic[4] phases have been proposed as the structural molecular arrangement for TAGS in the liquid phase. Although the actual structural mesophase organization of TAGS has not been established, all the work mentioned above agrees on the fact that TAGS molecules are somehow structured in a liquid crystalline-like state. Recently, we reported the pre-nucleation behavior of tripalmitin (TP) and tristearin (TS) in blends with triolein (TO), high oleic safflower oil (HOSfO), and soybean oil (SBO) as evaluated through anisotropy measurements and molecular mechanics simulations[5]. The TP/HOSfO and TP/SBO blends showed an increase in anisotropy, a behavior directly associated to an increase in the microviscosity of the blend that we interpreted as a structuring of TAGS before nucleation and growth of the crystals. A similar but less pronounced effect was also observed in the TS/SBO blends, but here the increase in anisotropy occurred after nucleation. This behavior was not observed in the TP/TO and the TS/TO blends[5]. We performed molecular mechanics simulations in an attempt to understand the molecular interactions responsible for this behavior. The simulation results indicated that the presence of TAGS molecules containing at least one chain of palmitic acid is a requisite to induce a molecular interaction through van der Waals forces with TP or TS, and therefore a pre-nucleation structuring of TAGS with the subsequent increase in the anisotropy, and therefore, in the microviscosity of the blends.

Within this framework, we investigated the molecular interaction occurring among TAGS before their nucleation, and its possible involvement in determining the activation free energy to develop a stable nucleus (ΔG_c). As in our previous study[5], the same TP and TS blends with TO, HOSfO, and SBO were used in the present investigation. The Fisher-Turnbull equation was utilized to calculate the ΔG_c using the induction time of crystallization (t_i) of the blends determined by differential scanning calorimetry (DSC) at different crystallization temperatures. To understand the behavior of ΔG_c in the blends, we performed an additional analysis of the anisotropy behavior in the blends to the one already done in our previous study[5]. The crystallization temperatures were selected in such a way to obtain similar supercooling conditions in all the blends investigated. As previously indicated[5], the blends investigated provided different degrees of molecular compatibility among the saturated TAGS (i.e., TP or TS) and the TAGS present in TO, HOSfO, and SBO. This since, in TO the major TAGS present was OOO (>99%), while in HOSfO were mainly OOO (≈66%), OOL (≈16%), POO (≈8.7%), and PLO (≈1.6%), and in SBO≈56% of TAGS were OOO, OOL, LLL, and LLO and ≈27% were POO, PLO, and LLP (where O=oleic acid, L=linoleic acid, and P=palmitic acid).

Materials and Methods

Blends Preparation

The TAGS, i.e., TP, TS, and TO, with purity higher than 99% were obtained from Sigma Chemical Co. (St. Louis, MO, USA). The HOSfO and the SBO were obtained from local manufacturers, their main TAGS composition has been reported previously[5]. Blends of each of the saturated TAGS (i.e., TP and TS) in TO, HOSfO, and SBO were prepared in a 25:75 (wt/wt) ratio as previously described[5].

Isothermal Crystallization

Based on dynamic thermograms obtained by DSC with a TA Instruments Model Q2000 (TA Instruments, New Castle, Delaware, USA) as described previously[5], different crystallization temperatures were established for isothermal crystallization studies. Thus, blend samples (6–8 mg) sealed in aluminum pans were heated (80°C/20 min) and then cooled to the corresponding crystallization temperature at 10°C/min. For each crystallized blend the melting temperature at the peak (T_M') was calculated with the equipment software using the first derivative of the heat flux[6]. With the T_M' values, the equilibrium melting temperature ($T_M°$) for TP and TS in the blends was determined following the procedure of Hoffman and Weeks[7], as described by Perez-Martinez et al.[8] and Toro-Vazquez et al.[9]. Based on the $T_M°$ values, crystallization temperatures (T_{Cr}) were selected in such a way to obtain similar supercooling conditions for all TP and TS blends investigated. The supercooling was calculated as $T_M°-T_{Cr}$. At each T_{Cr}, the induction time of crystallization (t_i) was determined with the equipment software using the first derivative of the heat flux. For the TP blends, the t_i was measured from 36°C to 41°C every degree, and for the TS blends from 46°C to 51°C every degree. In all cases, at least three independent determinations were obtained. The results were analyzed through ANOVA and contrast among the

treatment means using STATISTICA (V 9.0; StatSoft Inc., Tulsa, OK, USA).

Determination of ΔG_c

The Fisher-Turnbull equation was utilized to determine the magnitude of ΔG_c for the TP and the TS blends at each T_{Cr} investigated. The corresponding ΔG_c was calculated according to Ng[10] and Toro-Vazquez et al.[9] from the slope (s) of the linear regression of $\log[(t_i)/(T_{Cr})]$ vs. $1/T_{Cr}(T_M°-T_{Cr})^2$ through the following equation:

$$\Delta G_c = \mathrm{sk}/\left(T_M^{\circ} - T_{Cr}\right)^2$$

where, k is the Boltzmann constant. The results were statistically analyzed as in "Isothermal Crystallization" section.

Anisotropy Measurements

The anisotropy (r_s) of the blends was determined under the cooling and isothermal stages of the blends crystallization with a polarizer spectrophotometer (MD-5020 of Photon Technology International, London, ON, Canada) using the same time-temperature conditions as for t_i measurements (see "Isothermal Crystallization" section). We have described the details of the determination previously[5]. The r_s for the different TP and TS blends were plotted as a function of $T_M°-T_{Cr}$.

Results and Discussion

t_i and ΔG_c Analysis

The $T_M°$ for TP and TS in the three blends was 59.7°C (±0.83°C) and 70.2°C (±0.27°C), respectively (i.e., $T_M°$ for TP and TS was independent of the type of blend). As stated in the "Material and Methods" section, the T_{Cr}s selected for the isothermal crystallization studies provided similar supercooling (i.e., $T_M°-T_{Cr}$) conditions for TP and TS blends. Supercooling as calculated in the present manuscript, and supersaturation [Ln (β)] calculated as in our previous paper[5] (i.e., from the equality between the chemical potential equation and the Hildebrand equation), provided values of different magnitude but both measurements were highly correlated (Tables 1 and 2; $R^2>0.9830$, $P<0.001$).

The corresponding t_i and ΔG_c for the TP and TS blends as a function of supercooling are shown in Tables 1 and 2, respectively. At any given T_{Cr}, a single crystallization exotherm was always obtained that corresponded to the β polymorph for TP or TS crystallized in the blends (data not shown). X-ray analysis done to the blends[5] showed that at all T_{Cr}s investigated TP and TS crystallized in the β

Table 1 Induction time by DSC (t_i, min) at different supercooling ($T_M°-T_{Cr}$) used in the 25:75 (wt/wt) blends of tripalmitin (TP) or tristearin (TS) with triolein (TO), safflower oil high in triolein (HOSfO), or soybean oil (SBO). The Ln (β) is the prevailing supersaturation as calculated by Dibildox *et al.*[5]

$(T_M°-T_{Cr})$ Ln (β)	TP[d]			$(T_M°-T_{Cr})$ Ln (β)	TS[d]		
	TO	HOSfO	SBO		TO	HOSfO	SBO
23.7	2.04[a]	2.26[a]	2.08[a]	24.2	3.56[a]	4.76[b]	3.80[a]
0.26	(0.04)	(0.09)	(0.05)	0.24	(0.47)	(0.25)	(0.72)
22.7	2.50[a]	2.04[a]	2.85[b]	23.2	4.97[a]	5.08[a]	5.42[a]
0.24	(0.08)	(0.14)	(0.47)	0.22	(0.45)	(0.20)	(0.13)
21.7	2.66[a]	2.52[a]	3.30[b]	22.2	4.88[a]	5.73[a]	6.06[b]
0.22	(0.10)	(0.31)	(0.05)	0.21	(0.27)	(0.35)	(0.28)
20.7	2.61[a]	2.90[b]	3.70[c]	21.2	5.56[a]	5.42[a]	5.86[a]
0.21	(0.20)	(0.00)	(0.25)	0.19	(0.06)	(1.33)	(0.48)
19.7	2.98[a]	4.01[b]	4.48[c]	20.2	8.47[a]	6.64[b]	6.34[b]
0.19	(0.15)	(0.19)	(0.63)	0.17	(0.34)	(0.34)	(0.06)
18.7	4.79[a]	4.24[a]	5.09[b]	19.2	7.84[a]	8.14[a]	9.19[b]
0.18	(0.62)	(0.18)	(0.61)	0.17	(1.24)	(0.82)	(0.21)

[a, b, c]For the systems with TP or TS at the same $T_M°-T_{Cr}$, values with a different letter are statistically different ($P<0.10$). Values with the same letter are statistically the same

[d]Values are shown as the mean and standard deviation of at least two independent measurements

Table 2 Free energy for nucleation (ΔG_c) at different supercooling ($T_M°-T_{Cr}$) used in the 25:75 (wt/wt) blends of tripalmitin (TP) or tristearin (TS) with triolein (TO), safflower oil high in triolein (HOSfO), or soybean oil (SBO). The Ln (β) is the prevailing supersaturation as calculated by Dibildox *et al.*[5]

$(T_M°-T_{Cr})$ Ln (β)	TP[d]			$(T_M°-T_{Cr})$ Ln (β)	TS[d]		
	TO	HOSfO	SBO		TO	HOSfO	SBO
23.7	1.07[a]	1.48[b]	1.64[b]	24.2	2.01[a]	1.19[b]	1.67[b]
0.26	(0.29)	(0.09)	(0.20)	0.24	(0.27)	(0.17)	(0.34)
22.7	1.16[a]	1.61[b]	1.79[b]	23.2	2.19[a]	1.30[b]	1.82[b]
0.24	(0.32)	(0.10)	(0.22)	0.22	(0.30)	(0.19)	(0.37)
21.7	1.27[a]	1.76[b]	1.96[b]	22.2	2.39[a]	1.42[b]	1.98[b]
0.22	(0.35)	(0.11)	(0.24)	0.21	(0.33)	(0.20)	(0.40)
20.7	1.40[a]	1.94[b]	2.15[b]	21.2	2.62[a]	1.55[b]	2.17[b]
0.21	(0.38)	(0.12)	(0.27)	0.19	(0.36)	(0.22)	(0.44)
19.7	1.54[a]	2.14[b]	2.38[b]	20.2	2.88[a]	1.71[b]	2.40[b]
0.19	(0.42)	(0.13)	(0.29)	0.17	(0.39)	(0.25)	(0.49)
18.7	1.71[a]	2.37[b]	2.64[b]	19.2	3.19[a]	1.89[b]	2.65[b]
0.18	(0.47)	(0.14)	(0.33)	0.17	(0.44)	(0.27)	(0.54)

[a, b, c]For the systems with TP or TS at the same $T_M°-T_{Cr}$, values with a different letter are statistically different ($P<0.10$). Values with the same letter are statistically the same

[d]Values are shown as the mean and standard deviation of at least two independent measurements

polymorph (i.e., all diffractograms showed the characteristic peaks at ≈20, ≈23, and ≈24 2θ corresponding to the 4.6, 3.85, and 3.70 Å short spacings of the β polymorph). The linear regression of $\log[(t_i)/(T_{Cr})]$ vs. $1/T_{Cr}(T_M°-T_{Cr})^2$ provided in all cases determination coefficients (R^2) greater than 0.86 (i.e., $R>0.927$). As an example, Figure 1 includes Fisher-Turnbull plots for TP (Figure 1a) and TS (Figure 1b) blends, showing the corresponding R^2 and statistical significance of the regression equation. Thus, as has been shown by other authors [9-13], the Fisher–Turnbull equation, although originally developed for a single-component system, is applicable to complex TAGS systems as the TP and TS blends investigated.

Overall, for all blends investigated, t_i and ΔG_c increased as supercooling decreased (i.e., T_{Cr} increased). In general, for similar supercooling (and saturation), t_i was longer for TS blends than for TP blends. Thus, other factors besides supercooling must be considered to explain differences in the crystallization kinetics between homogenous saturated TAGS (i.e., TP vs. TS). For the TP blends and at all levels of supercooling investigated, t_i in the TP/SBO blend was the longest (Table 1) and ΔG_c increased following the order SBO>HOSfO>TO (Table 2). However, the ΔG_c for TP/SBO and TP/HOSfO blends were not statistically different at any of the T_{Cr} investigated ($P=0.25$; Table 2). In contrast, t_i in the TS blends did not show a particular trend and ΔG_c increased following the order TO>SBO>HOSfO. However, as observed in the TP blends, ΔG_c for TS/SBO and TS/HOSfO blends were not statistically different ($P=0.12$; Table 2). This indicated that under similar supercooling conditions, TP required more energy to nucleate in SBO and HOSfO than in TO, while TS nucleation required more activation energy in TO than in SBO and HOSfO. Within this framework, it is important to point out that in TO, the TS nucleation required approximately twice the activation energy than TP, while when blended with SBO and HOSfO, both TP and TS showed similar ΔG_c values.

Our previous study involving anisotropy and molecular mechanics simulations using the same blends[5] showed that the presence of TAGS molecules containing at least one chain of palmitic acid (i.e., POO) is a requisite to induce a molecular interaction through van der Waals forces with TP or TS, and therefore a pre-nucleation structuring of TAGS. According to the TAGS composition previously reported[5], no palmitic acid was present in TO, while palmitic acid was present in HOSfO and in SBO as LLP, PLO/POL, and POO. Then, the presence of TAGS containing palmitic acid in the blends made with HOSfO and SBO ought to induce a pre-nucleation structuring of TAGS. Comparing the ΔG_c for the blends made with TO, the TAGS structuring occurring before nucleation (i.e., in the liquid state) resulted in a higher energy requirement for TP nucleation in the blends made with HOSfO and SBO (Table 2). In contrast, TS nucleation in HOSfO and SBO required a lower ΔG_c than in the TS/TO blend.

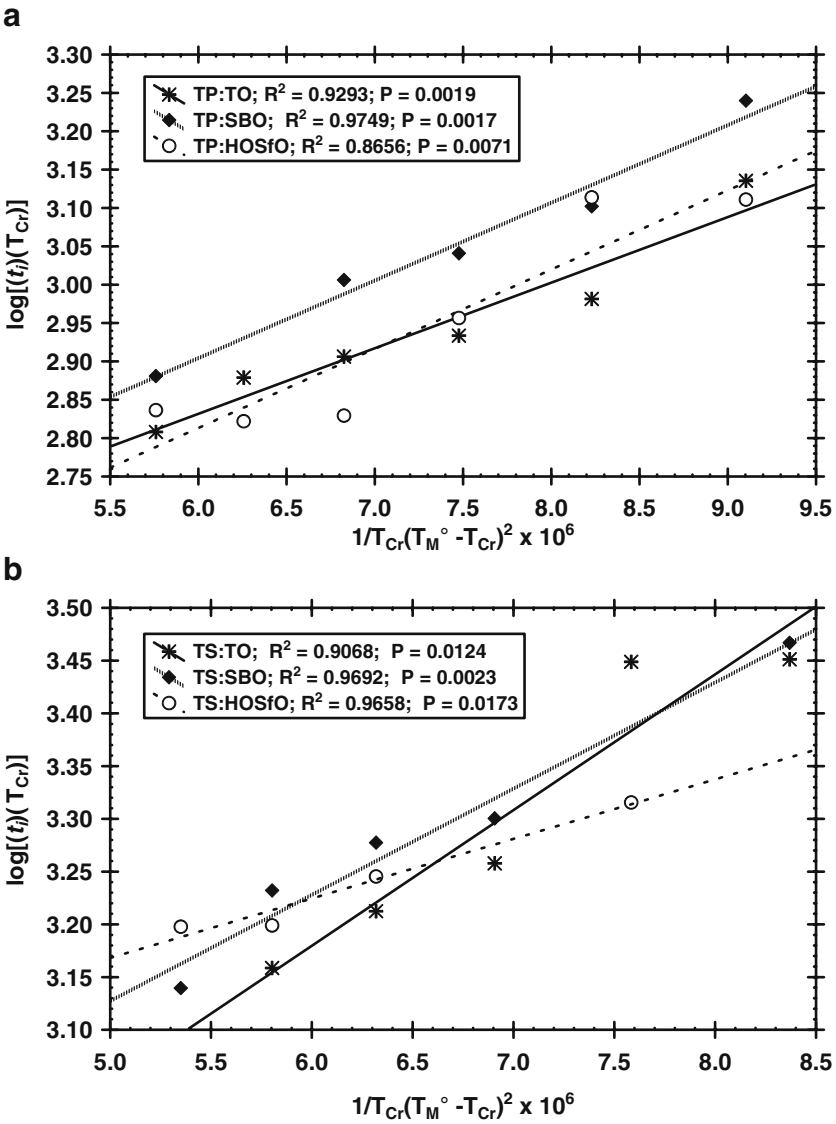

Fig. 1 Fisher-Turnbull plots for TP (**a**) and TS (**b**) blends with TO, HOSfO, and SBO. The legend shows the corresponding determination coefficient (R^2) and statistical significance (P) of the linear regression equation

Anisotropy Behavior under Cooling and Isothermal Conditions

The organization of TAGS in the blends might be evaluated by the evolution of r_s as the system is cooled to achieve isothermal conditions. The development and attainment of critical number of TAGS molecules structured in a liquid state or mesophase is a requirement to achieve TAGS nucleation. All the works associated with proposing molecular arrangements for TAGS melts agrees on this[2-4, 14-17]. In fact, the change in TAGS viscosity with temperature is determined by the shape and size of the TAGS liquid structures[18] that is indirectly measured by r_s. Within this framework, in an attempt to understand the behavior of ΔG_c in the blends, Figure 2 shows the behavior of r_s in the blends as a function of supercooling during the cooling and isothermal stages. The r_s value for the isothermal stage plotted in Figure 3 was obtained once T_{Cr} was attained and corresponds to the average of r_s values obtained during the first 60 s under isothermal conditions (i.e., before t_i was achieved in the blend).

During the cooling stage, all blends investigated showed an exponential increase of r_s (i.e., TAGS achieved a higher level of liquid structure) as supercooling increased (R^2>0.95; Figure 2). Nevertheless, TP and TS blends showed some distinctive features of how r_s changed as a function of supercooling. Thus, all TP blends observed similar r_s values and its change as a function of supercooling was independent of the type of blend [i.e., the same equation fitted the r_s vs. ($T_M°-T_{Cr}$) data for the three TP blends; $r_s=0.0236\times\exp[0.0331\times(T_{Cr}-T_M°)]$, $R^2=0.9914$]. In the same way, TAGS in the liquid state were more structured in the TP blends than in the TS blends (i.e., overall TS blends showed lower r_s values than the TP

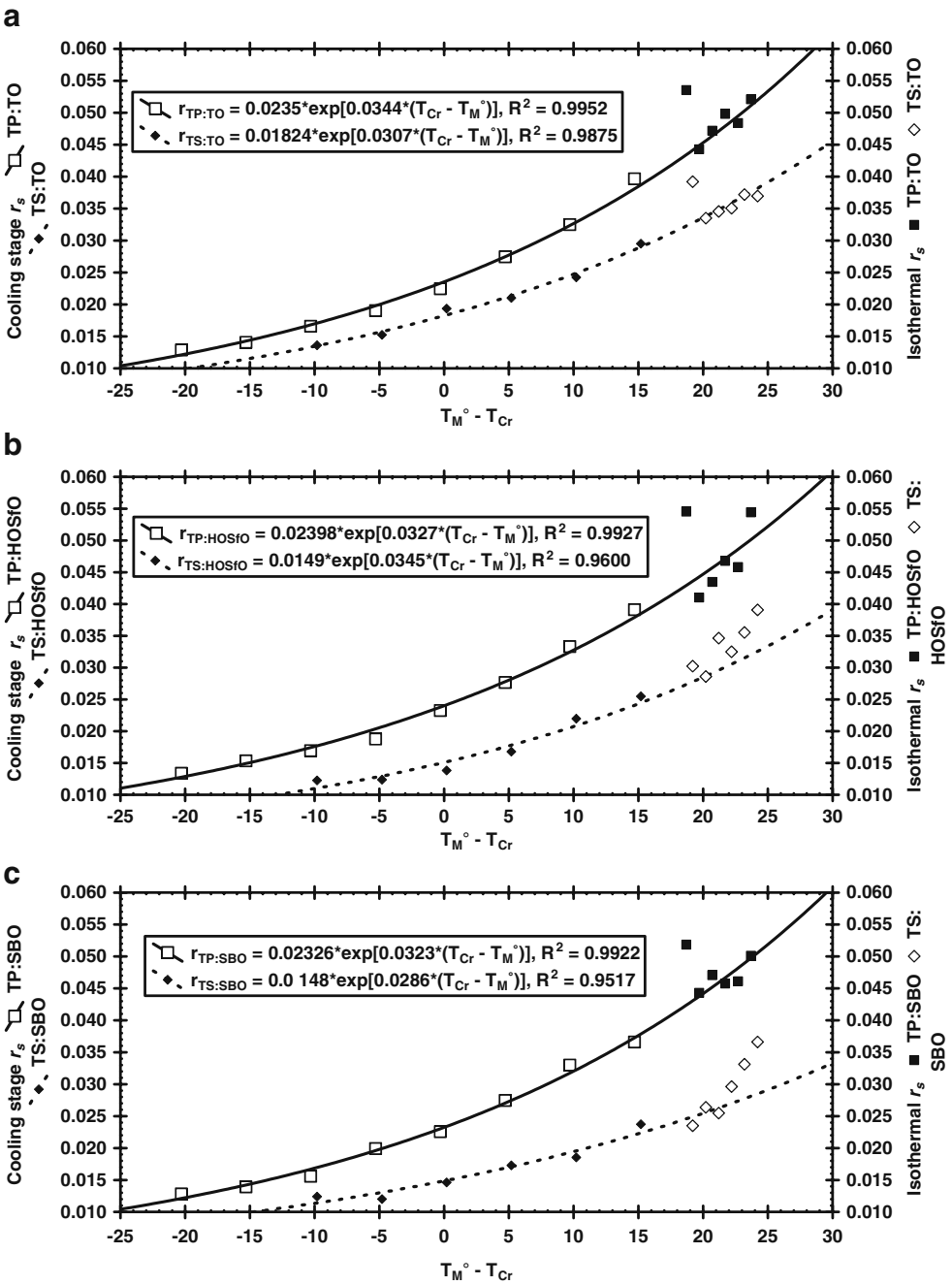

Fig. 2 r_s as a function of supercooling for the TP and TS blends with TO (**a**), HOSfO (**b**), and SBO (**c**) during the cooling stage and at the T_{Cr} used for isothermal crystallization. The fitting equations show considered r_s values just during the cooling stage

blends). Additionally, in the TS blends the r_s values showed the following order TO>HOSfO>SBO. However, as observed for ΔG_c, the r_s values for TS/SBO and TS/HOSfO blends were not statistically different.

From the above, we conclude that during the cooling stage, the addition of TP to TO, HOSfO, and SBO did not modify the original TAGS liquid structure. Such behavior was followed for all TP blends at the different T_{Cr}s used for isothermal crystallization (Figure 2). In contrast, the addition of TS resulted in decreasing the TAGS liquid structure particularly in the TS/HOSfO and TS/SBO blends. Additionally, except for the TS/TO blend, r_s in the TS/HOSfO and TS/SBO blends showed a significant change in the slope once isothermal conditions were achieved (Figure 2). This change in the behavior of r_s at such supercooling conditions (i.e., T_{Cr}s $\leq$51 °C), was associated with the developing of a higher TAGS structural organization than the one anticipated by the exponential fitting of r_s during the cooling stage (Figure 2). Thus, before t_i was achieved TAGS in the TS/HOSfO and TS/SBO blends accomplished a particular structural organization. Since the TS/TO blend did not show this change in the slope (Figure 2), TAGS structuring in the liquid state was not associated to triolein.

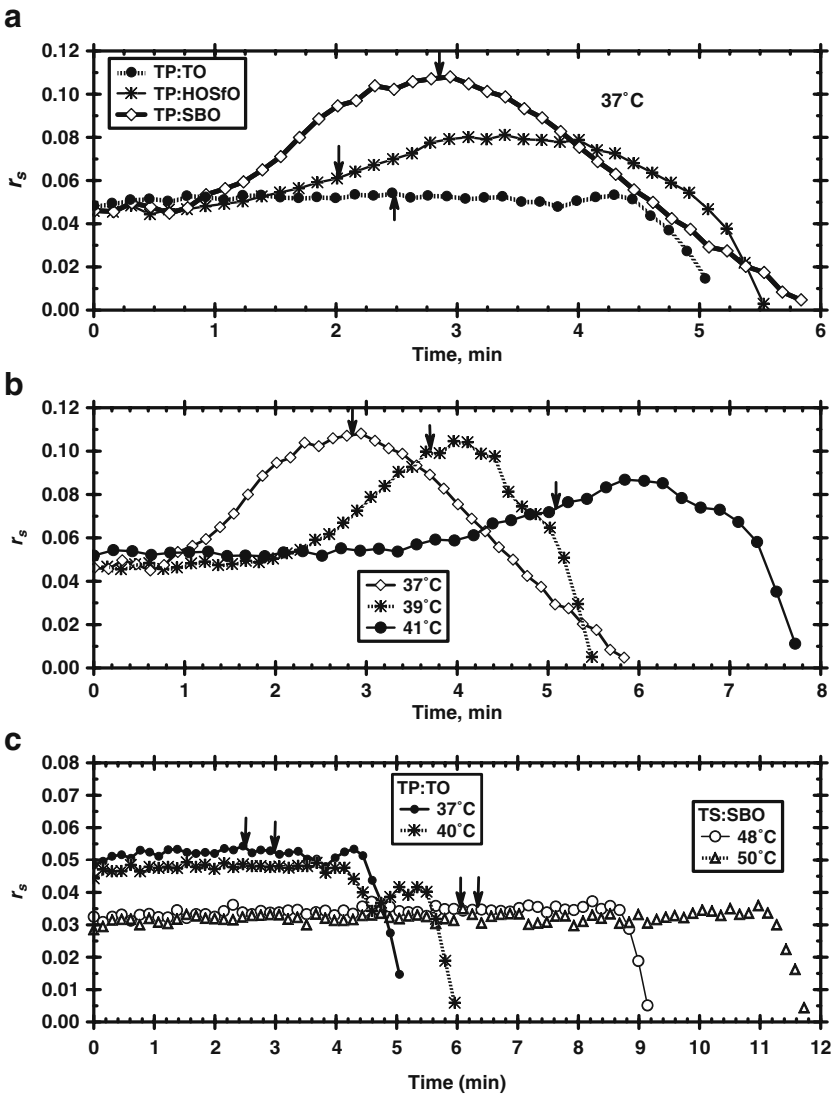

Fig. 3 Evolution of r_s under isothermal conditions for TP/TO, TP/HOSfO, and TP/SBO blends at a T_{Cr}=37°C (**a**), TP/SBO blends (**b**), TP/TO and TS/SBO blends (**c**) at different T_{Cr}. The *arrows* indicate the induction time for crystallization (t_i) for the corresponding blends

According to the TAGS analysis previously reported[5], HOSfO had about 10% of TAGS containing palmitic acid in their composition whereas SBO had approximately 30% of these TAGS. Thus, the lower r_s values observed in the TS/HOSfO and TS/SBO blends in comparison with the ones observed in the TS/TO blend and the extent of change in the slope observed in the TS blends (Figure 2), might be associated with the concentration of TAGS containing palmitic acid present in the blend. Thus, a more pronounced slope change was observed in the TS/SBO blend than in the TS/HOSfO, and no change was observed in the TS/TO blend. The molecular interaction of TS with POO, LLP, and PLO/POL seems to occur well before achieving supercooling conditions that resulted in TAGS crystallization (i.e., during the cooling stage). TO, HOSfO, and SBO do not contain TAGS with stearic acid, and since stearic acid has a longer hydrocarbon chain length than palmitic acid, structural compatibility between TAGS containing palmitic acid and TS was not effective. The result was a decrease in TAGS liquid structure and therefore, lowers r_s values in the TS/HOSfO and TS/SBO blends. Once supercooling conditions required for TAGS crystallization were prevalent (i.e., T_{Cr}s≤51 °C), palmitic acid present in the TAGS facilitated TS nucleation. As a result, ΔG_c was lower in the TS/HOSfO and TS/SBO blends compared with the activation energy required by TS in the TS/TO blend (Table 2). Probably, under such supercooling conditions, TAGS with palmitic acid acted as template for TS structuring in the liquid state and from here the change in the slope of the r_s vs. (T_M°−T_{Cr}) relationship in the TS/SBO and TS/HOSfO blends (Figure 2). The result was a lower ΔG_c for TS crystallization in SBO and HOSfO, in comparison with the ΔG_c observed in the TS/TO blend (Table 2).

Once under isothermal conditions, the r_s values in all TS blends remained constant as a function of time until t_i was achieved (i.e., no solid phase was present). This

behavior was observed at all T_{Cr}s investigated. Examples of such behavior are presented for the TS/SBO blend at the T_{Cr} of 48 °C and 50 °C in Figure 3c. The decrease in r_s observed after nucleation (i.e., after t_i; Figure 3) was associated to light scattering from the nuclei developed. In some cases (i.e., TS/TO at 49 °C and 50 °C and TP/TO at 39 °C and 40 °C; results not shown), after t_i, we observed an increase in r_s before decreasing. In our previous paper [5], we associate this behavior as a structuring of TAGS due to molecular interaction between TS and TAGS containing palmitic acid. However, since this r_s peak occurred right after nucleation, the behavior might be associated to remelting of the solid phase due to the heat generated during TAGS crystallization with the subsequent increase in r_s. As crystallization continued and more solid phase was present, light scattering produced a decrease in r_s.

In contrast to the TS blends, the TP/SBO and TP/HOSfO blends showed an increase in r_s as a function of time under isothermal conditions. The increase in r_s (i.e., TAGS structuring) was a direct function of the concentration of TAGS containing at least one chain of palmitic acid, i.e., the increase in r_s followed the order TP/SBO>TP/HOSfO and no increase in the TP/TO blend (Figure 3a). For the TP/HOSfO (data not shown) and the TP/SBO (Figure 3b) blends, the r_s onset was an inverse function of supercooling, and the extent of its increment was a direct function of supercooling. Thus, the molecular interaction of TP with POO, LLP, and PLO/POL were time and temperature dependent. Such molecular interactions seem to make TP nucleation more difficult in the TP/SBO and TP/HOSfO blends than in the TP/TO blend. As a result ΔG_c was higher in TP/SBO and TP/HOSfO blends when compared with the ΔG_c in the TP/TO blend (Table 2). Mihara et al.[19] showed that mixtures of TP and POO crystallize more slowly that the pure TAGS. This regardless an independent crystallization of TP and POO was observed in the mixture (i.e., no mixed crystal formation occurred)[19]. Probably, the molecular interactions occurring in the liquid phase between TP and TAGS with palmitic acid resulted in the development of a mixed TAGS lamellar liquid structure. This would delay the nucleation of TP, until segregation of TP from the mixed TAGS lamellar liquid structure occurred. The result was a higher ΔG_c for TP nucleation as the concentration of TAGS with palmitic acid (i.e., LLP, POO, PLO, and PLO) increased in the blends (Table 2).

Acknowledgments The investigation was supported by grant #25706 from CONACYT. We acknowledge and appreciate the fellowship from PROMEP for Elena Dibildox-Alvarado through the grant PROMEP/103.5/05/1624. The technical support from Concepcion Maza-Moheno and Elizabeth Garcia-Leos is greatly appreciated.

References

1. D. Pérez-Martínez, C. Alvarez-Salas, M.A. Charo-Alonso, E. Dibildox-Alvarado, J.F. Toro-Vazquez, The cooling rate effect on the microstructure and rheological properties of blends of cocoa butter with vegetable oils. Food Research International **40**, 47–62 (2007). doi:10.1016/j.foodres.2006.07.016
2. D.J. Cebula, D.J. McClements, M.J.W. Povey, P.R. Smith, Neutron diffraction dtudies of liquid and crystalline trilaurin. Journal of the American Oil Chemists' Society **69**, 130–136 (1992). doi:10.1007/BF02540562
3. K. Larsson, Molecular arrangement in glycerides. Fette, Seifen, Anstrichmittel **74**, 136 (1972). doi:10.1002/lipi.19720740302
4. R.W. Corkery, D. Rousseau, P. Smith, D.A. Pink, C.B. Hanna, A case for discotid liquid crystals in molten triglycerides. Langmuir **23**, 7241–7246 (2007). PMID: 17511482
5. Dibildox-Alvarado, E., Laredo, T., Toro-Vazquez, J. F., Marangoni, A. G. Pre-nucleation structuring of TAG melts revealed by fluorescence polarization spectroscopy and molecular mechanics simulations, Journal of the American Oil Chemists' Society (2010). doi:10.1007/s11746-010-1596-8
6. J.F. Toro-Vazquez, E. Dibildox-Alvarado, M.A. Charó-Alonso, V. Herrera-Coronado, C.A. Gómez-Aldapa, The Avrami index and the fractal dimension in vegetable oil crystallization. Journal of the American Oil Chemists' Society **79**, 855–866 (2002). doi:10.1007/s11746-002-0570-y
7. J.D. Hoffman, J.J. Weeks, Melting process and the equilibrium melting temperature of polychlorotrifluoroethylene. Journal of Research of the National Bureau of Standards **66**, 13–28 (1962)
8. D. Pérez-Martínez, C. Alvarez-Salas, J. Morales-Rueda, J.F. Toro-Vazquez, M. Charó-Alonso, E. Dibildox-Alvarado, The effect of supercooling on crystallization of cocoa butter-vegetable oil blends. Journal of the American Oil Chemists' Society **82**, 471–479 (2005). doi:10.1007/s11746-005-1096-z
9. J.F. Toro-Vazquez, M. Briceño-Montelongo, E. Dibildox-Alvarado, M.A. Charó-Alonso, J. Reyes-Hernández, Crystallization kinetics of palm stearin in blends with sesame seed oil. Journal of the American Oil Chemists' Society **77**, 297–310 (2000). doi:10.1007/s11746-000-0049-x
10. W.L. Ng, A Study of the kinetics of nucleation in a palm oil melt. Journal of the American Oil Chemists' Society **67**, 879–882 (1990). doi:10.1007/BF02540510
11. J.W. Litwinenko, A.M. Rojas, L.N. Gerschenson, A.G. Marangoni, Relationship between crystallization behavior, microstructure, and mechanical properties in a palm oil-based shortening. Journal of the American Oil Chemists' Society **79**, 647–654 (2002). doi:10.1007/s11746-002-0538-y
12. C.W. Chen, O.M. Lai, H.M. Ghazali, C.L. Chong, Isothermal crystallization kinetics of refined palm oil. Journal of the American Oil Chemists' Society **79**, 403–410 (2002). doi:10.1007/s11746-002-0496-4
13. M. Cerdeira, V. Pastore, L. Vera, S. Martini, R.J. Candal, M.L. Herrera, Nucleation behavior of blended high-melting fractions of milk fat as affected by emulsifiers. European Journal of Lipid Science and Technology **107**, 877–885 (2005). doi:10.1002/ejlt.200500257
14. A. Minato, S. Ueno, K. Smith, Y. Amemiya, K. Sato, Thermodynamic and kinetic study on phase behavior of binary mixtures of POP and PPO forming molecular compound systems. The Journal of Physical Chemistry. B **101**, 3498–3505 (1997). doi:10.1021/jp962956v
15. S. Ueno, A. Minato, J. Yano, K. Sato, Synchrotron radiation X-ray diffraction study of polymorphic crystallization of SOS from liquid phase. Journal of Crystal Growth **198**, 1326–1329 (1999). doi:10.1016/S0022-0248(98)01018-5

16. K. Larsson, On the structure of the liquid state of triglycerides. Journal of the American Oil Chemists' Society **69**, 835–836 (1992). doi:10.1007/BF02635928
17. L. Hernqvist, On the structure of triglycerides in the liquid state and fat crystallization. Fette Seifen Anstrichmittel **86**, 297 (1984)
18. J.F. Toro-Vazquez, A. Gallegos-Infante, Viscosity and its relationship to crystallization in a binary system of saturated triacylglycerides and sesame seed oil. Journal of the American Oil Chemists' Society **73**, 1237–1246 (1996). doi:10.1007/BF02525452
19. H. Mihara, T. Ishiguro, H. Fukano, S. Taniuchi, K. Ogino, Effect of crystallization temperature of palm oil on Its crystallization. IV. The influence of tripalmitoylglycerol (PPP) on the crystallization of 1, 3-dipalmitoyl-2-oleoyl-glycerol (POP) and 1, 2, dioleoyl -3-palmitoyl-glycerol (POO). Journal of Oleo Science **56**, 223–230 (2007). PMID: 17898485